

POSITION AND SPEED CONTROL OF ELECTROMECHANICAL ACTUATOR FOR AEROSPACE APPLICATIONS

Ivana Todić, Marko Miloš, Mirko Pavišić

Original scientific paper

Main focus of this paper is control of electromechanical actuator (EMA) for aerospace applications. Control of EMA done using position regulator and control which combine position and speed regulator is shown. The main guideline is to decrease power losses, heating and current consumption in the system. One of the important areas within the field of variable speed motor drives are the system's operational boundaries. Presently, the operational boundaries of variable speed motor drives are set based on the operational boundaries of single speed motors, i.e. by limiting current and power to rated values. This results in under-utilization of the system, and places the motor at risk of excessive power losses. In this paper, the first part represents general concept of electromechanical actuators and mathematical modelling of the system; then the control of position and speed of electromechanical actuator (EMA) by using PID controller is presented. The second part shows simulations of our own design of control speed and position by PID controller using SIMULINK and MATLAB software.

Keywords: brushless DC motor, electromechanical actuator (EMA), PID controller, position control, speed control, simulations

Upravljanje položajem i brzinom elektromehaničkog aktuatora (EMA) za primjene u zračnom prostoru

Izvorni znanstveni članak

Težište ovog rada je upravljanje elektromehaničkim aktuatorom (EMA) za primjene u zračnom prostoru. Upravljanje EMA je ostvareno uporabom pozicijskog regulatora i upravljanja koje kombinira položaj i brzinu regulatora. Osnovna smjernica bila je smanjenje gubitaka snage, zagrijavanja i potrošnje struje u sustavu. Jedno od važnih područja u okviru pogona promjenljivim brzinama motora su operativne granice sustava. Danas se operativne granice pogona s promjenljivim brzinama motora postavljaju na osnovu operativnih granica pogona na bazi prosječnih vrijednosti, npr. ograničenjima struje i snage na preporučene vrijednosti. To dovodi do nedovoljne iskorištenosti sustava i velikih gubitaka korisne snage. U ovom radu, u prvom dijelu je predstavljen osnovni koncept elektromehaničkog aktuatora (EMA) i njegov matematički model, zatim je prikazano upravljanje položajem i brzinom elektromehaničkog aktuatora uporabom PID regulatora. U drugom dijelu usporedo se daje prikaz simulacija vlastite konstrukcije upravljanja položajem i brzinom pomoću PID regulatora, uporabom SIMULINK-a u MATLAB-u.

Ključne riječi: DC motor bez četkica, elektromehanički aktuator (EMA), PID regulator, pozicijsko upravljanje, brzinsko upravljanje, simulacije

1 Introduction

In reference to the literature ([1, 2] and many others not cited here), for the better part of 20th century most motion control systems were designed to operate at a fixed speed.

Many existing systems still operate based on a speed determined by the frequency of the power grid. However, the most efficient operating speed for many applications, such as fans, blowers and centrifugal pumps, is different from that enforced by the grid frequency. Also, many high performance applications, such as robots, machine tools and the hybrid vehicle, require variable speed operation to begin with. As a result, a major transition from single speed systems to variable speed systems is in progress.

The transition from single speed drives to variable speed drives has been in effect since the 1970s when movements towards conservation of energy and protection of the environment were initiated. About seventy percent of all electrical energy is converted into mechanical energy by motors in the industrialized world.

This may be the most important factor behind today's high demand for more efficient motion control systems. A large body of research is available on variable speed drives due to the significant industrial and commercial interest in such systems.

However, some areas of importance merit further investigation. One such area is the operational boundary of motor drives. The operational boundaries of variable speed motor drives are being incorrectly set based on the

operational boundaries of single speed motor drives, i.e. by limiting current and power to rated values.

The operational boundary of any motor drive must be set based on the maximum possible power loss vs. speed profile for the given motor.

Also, all control strategies for a machine must be analysed and compared based on such an operational boundary [3].

2 General concept and mathematical model of EMA

Linear actuator is a device that applies force in a linear manner, as opposed to rotationally like an electric motor. Electro-mechanical actuators are similar to mechanical actuators except that the control knob or handle is replaced with an electric motor. Rotary motion of the motor is converted to linear displacement of the actuator.

The main equation used to describe electro-mechanical actuator is based on Euler equation and Faraday's law:

$$J \frac{d\omega_r}{dt} = T_e - T_m - F \cdot \omega_r. \quad (1)$$

The angular position may be obtained by integration of the angular velocity:

$$\theta_r = \int \omega_r dt. \quad (2)$$

Now we need to introduce equations to describe relationship between current, voltage, and back electromotive force and rotor velocity [4, 5]. Next equations are expressed in the phase reference frame (ABC frame):

$$\begin{aligned} L_s \frac{di_a}{dt} + R_s \cdot i_a &= \frac{1}{3} [2v_{ab} + v_{bc} + p \cdot \lambda \cdot \omega_r (-2\Phi'_a + \Phi'_b + \Phi'_c)] \\ L_s \frac{di_b}{dt} + R_s \cdot i_b &= \frac{1}{3} [-v_{ab} + v_{bc} + p \cdot \lambda \cdot \omega_r (\Phi'_a - 2\Phi'_b + \Phi'_c)] \\ \frac{di_c}{dt} &= -\left(\frac{di_a}{dt} + \frac{di_b}{dt}\right). \end{aligned} \quad (3)$$

Generated electromagnetic torque is given by:

$$T_e = p \cdot \lambda \cdot (\Phi'_a \cdot i_a + \Phi'_b \cdot i_b + \Phi'_c \cdot i_c), \quad (4)$$

where [6, 7]:

- sinusoidal flux distribution

$$\lambda = K_a \cdot \frac{\sqrt{2}}{3p}, \quad (5)$$

- trapezoidal flux distribution

$$\lambda = \frac{K_a}{2p}. \quad (6)$$

DC motor which was under our consideration has trapezoidal flux distribution. The following equations will be used for calculation of electromotive force:

$$\begin{aligned} \Phi'_a &= \frac{C_a}{trap}, \\ C_a &= f(\cos\theta_e), \\ f(\cos\theta_e) &= \begin{cases} \cos\theta_e; & -trap \leq \cos\theta_e \leq trap \\ \text{sgn}(\cos\theta_e) \cdot trap; & |\cos\theta_e| > trap \end{cases} \\ trap &= \sin\left(\frac{\pi\left(1 - \frac{flat}{180}\right)}{2}\right), \end{aligned} \quad (7)$$

where:

flat – back EMF flat area [degrees]. We can use sinusoidal flux distribution if we set *flat* = 0.

Electrical angle is:

$$\theta_e = p \cdot \theta_r, \quad (8)$$

$$\Phi'_b = \frac{C_b}{trap},$$

$$C_b = f\left[\cos\left(\theta_e - \frac{2\pi}{3}\right)\right], \quad (9)$$

$$\Phi'_c = \frac{C_c}{trap},$$

$$C_c = f\left[\cos\left(\theta_e + \frac{2\pi}{3}\right)\right].$$

Load torque is calculated as sum of coulomb friction of motor, load torque and coulomb and viscous friction in gearbox:

$$T_m = T_f + T_A + T_{gf} + T_{gv}. \quad (10)$$

All those equations are implemented in SIMULINK model to simulate electromechanical actuator system.

3 Control of EMA

Usually pulse-width modulation circuit is used for control of DC brushless motor in EMA applications. The pulse-width modulation signals are generated according to polarity and intensity of input signals. The bridge power driving circuit applies different voltages to two ends of the motor according to the input signal to rotate the motor shaft in different directions. Input signal in pulse-width modulation circuit is the result of PID control of desired signal (position/deflection or desired speed). We will compare control of EMA based on position controller and combined controller which simultaneously control position and speed.

3.1 Position controller and dynamic characteristics

The main guideline of control of DC brushless motor (as a major part of EMA) is to control its input current. For calculation of suitable PID position controller we will need to determine transfer function of EMA system [ref. Chapter 4 of this paper].

It will be assumed that DC brushless motor can be presented by equivalent electric circuit [8, 9, 10] (Fig 1).

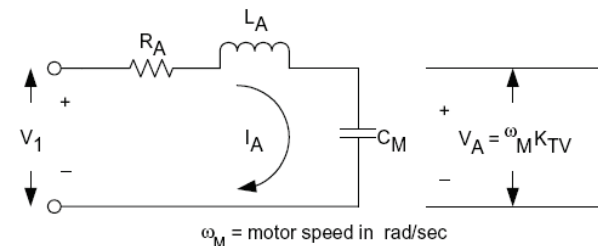


Figure 1 Schematic of motor model presented by equivalent electric circuit

where:

$$C_M = \frac{J}{K_a^2}, \quad (11)$$

J – Total inertia, inertia of motor and its load, kg·m²

K_a – Torque constant, (N·m)/A

G – Gearbox ratio

R_A – Resistance in phase A, Ω

L_A – Inductance in phase A, H

I_A – Current in phase A, A

V_A – Back EMF in phase A, V

V₁ – Power supply, V.

The transfer function for the motor:

$$\theta = \frac{1}{G \cdot s} \cdot \omega,$$

$$\omega \cdot K_v = V = \frac{I}{C \cdot s},$$

$$\Rightarrow \frac{\omega}{I} = \frac{1}{K_a \cdot C \cdot s} = \frac{1}{K_a \cdot \frac{J}{K_a^2 \cdot s}} = \frac{K_a}{J \cdot s}, \quad (12)$$

$$\Rightarrow H_M(s) = \frac{\theta}{I} = \frac{K_a}{J \cdot G \cdot s^2}.$$

The transfers function for PID regulator:

$$H_{PID}(s) = A_0 \cdot \frac{K_i + K_p \cdot s + K_d \cdot s^2}{s}. \quad (13)$$

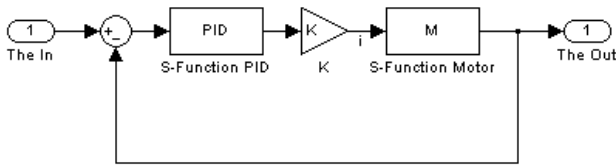


Figure 2 Block diagram of DC brushless motor and position PID regulator

The transfer function for the actuator system can be written as [11]:

$$H(s) = \frac{H_{PID}(s) \cdot H_M(s)}{1 + H_{PID}(s) \cdot H_M(s)}, \quad (14)$$

$$H(s) = \frac{\frac{K_d}{K_i} \cdot s^2 + \frac{K_p}{K_i} \cdot s + 1}{\frac{G \cdot J}{K_i \cdot A_0 \cdot K_a \cdot K} \cdot s^3 + \frac{K_d}{K_i} \cdot s^2 + \frac{K_p}{K_i} \cdot s + 1}. \quad (15)$$

Using MATLAB calculation we can obtain $H(s)$ of our electromechanical actuator system:

$$H(s) = \frac{0,5418 \cdot s^2 + 72,24 \cdot s + 36,12}{0,005787 \cdot s^3 + 0,5418 \cdot s^2 + 72,24 \cdot s + 36,12}. \quad (16)$$

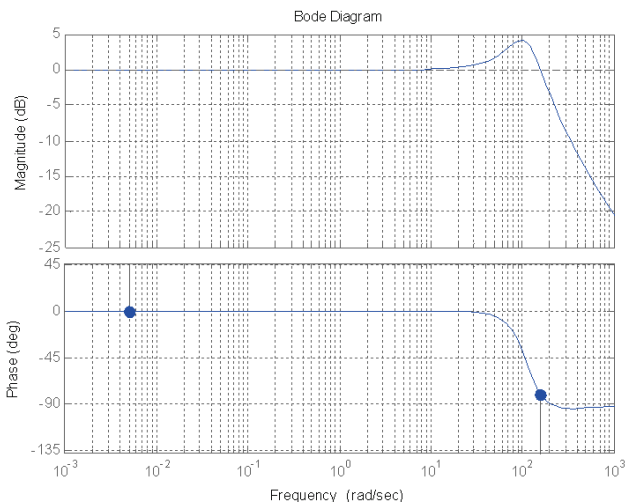


Figure 3 Bode diagram of position controller

3.2 Combined regulator, position and speed controller

The main guideline is to impose some additional control on the same system. Position PID regulator will stay unchanged. Imposed component is output signal from the speed controller. Speed controller will take effect on the whole system like additional differential component so coefficients in speed controller need to be the same order like differential component in position controller.

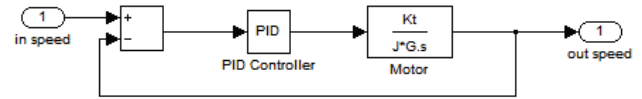


Figure 4 Block diagram of DC brushless motor and speed PID regulator

The general transfer function for PID regulator and position controller is:

$$H_{Ms}(s) = \frac{\theta}{I} = \frac{K_a}{J \cdot G \cdot s^2}, \quad (17)$$

$$H_{PIDs}(s) = A_0 \cdot \frac{K_i + K_p \cdot s + K_d \cdot s^2}{s}, \quad (18)$$

$$H_s(s) = \frac{H_{PID}(s) \cdot H_M(s)}{1 + H_{PID}(s) \cdot H_M(s)}. \quad (19)$$

Using MATLAB calculation we can obtain $H_s(s)$ of our electromechanical actuator system:

$$H_s(s) = \frac{4,515 \times 10^{-5} \cdot s^2 + 1,129 \cdot s + 0,7224}{0,005832 \cdot s^2 + 1,129 \cdot s + 0,7224}. \quad (20)$$

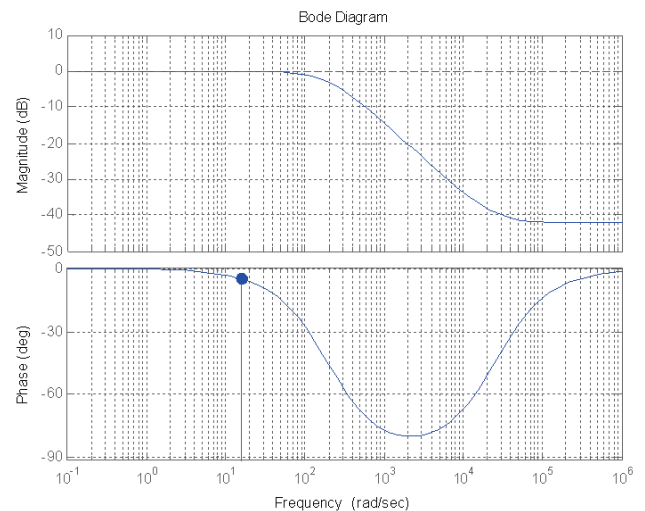


Figure 5 Bode diagram of speed controller

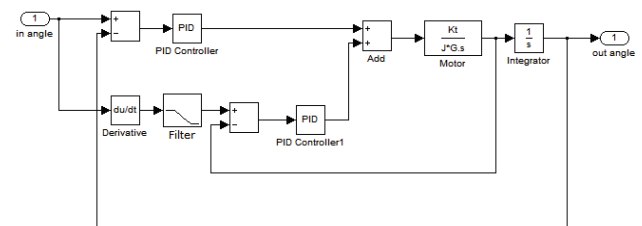


Figure 6 Block diagram of DC brushless motor and combined position and speed regulator

Combined regulator will be based on sum of responses of both position and speed regulators.

4 Model of EMA

Model of EMA used in simulations is presented in Fig. 7. Main parts are: Object /Fin (1), Lever mechanism (2), Planetary roller screw (3), Gearhead (4) and DC brushless motor (5). Controller consists of driver and DSP.

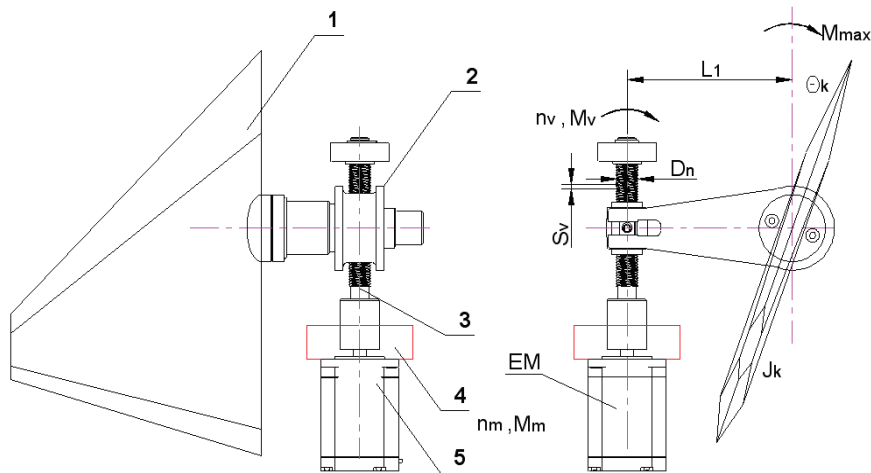


Figure 7 Rough schematic of EMA used in the simulations (n_m, M_m – Rated speed and torque of motor, n_v, M_v – Rated speed and torque of planetary roller screw, L_1 – Lever arm length, S_v – Lead, D_n – Nominal diameter, J_k – Inertia of control surface, θ_k – Deflection of control surface, M_{max} – Maximum output torque)

5 Results

In this paper, SIMULINK is used for design of PID controller for both position and velocity controller of EMA and for modelling of EMA system.

To illustrate the above mentioned, several series of results follow as well as Simulink schematic of electro-mechanical system (Fig. 8).

Simulation results on input signal 0,1 deg 6 Hz used to compare small signal bandwidth of both systems (Fig. 9 to Fig. 12). Simulation results on input signal 6 deg 3 Hz used to compare response of both systems on maximum requirements (Fig. 13 to Fig. 16). Simulation results on two different input signals based on guidance algorithm and autopilot, used to compare response of both system in realistic conditions (Fig. 17 to Fig. 20).

Brushless DC motor fed by six step inverter

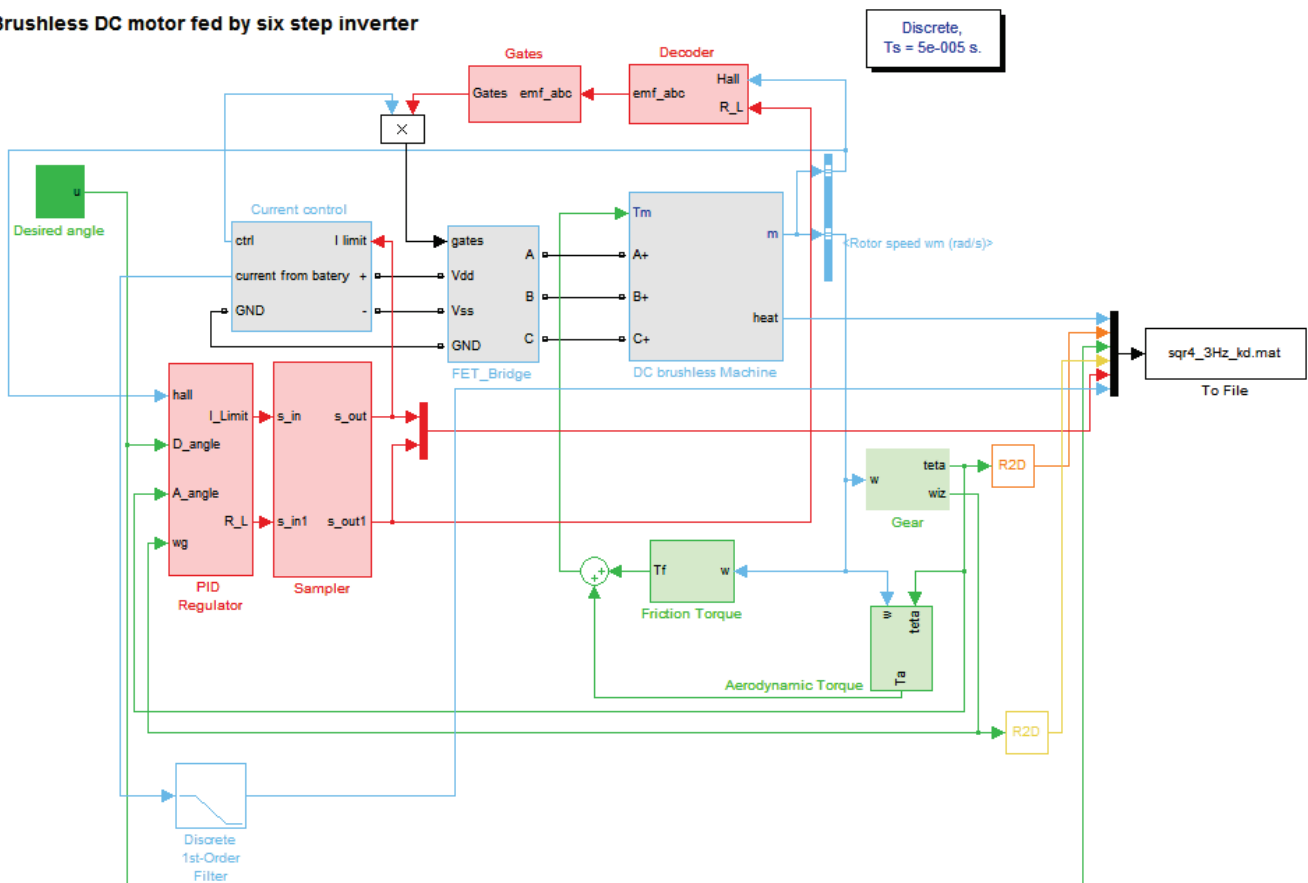


Figure 8 SIMULINK schematic of EMA

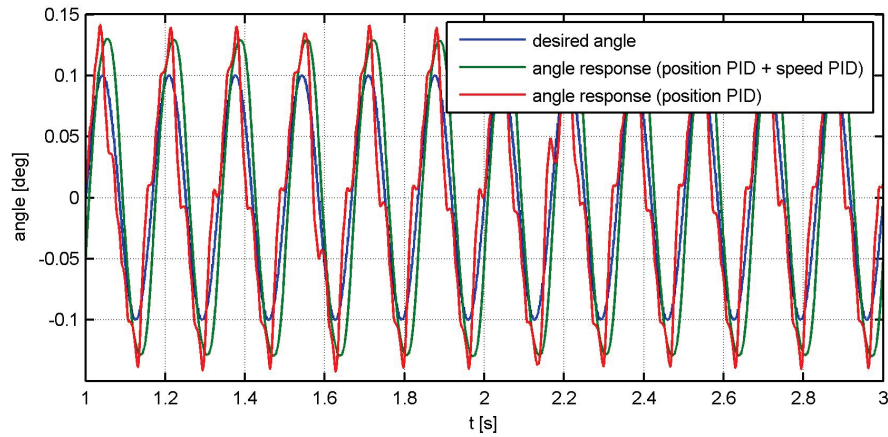


Figure 9 Angle responses of position controller and combined position + speed controller

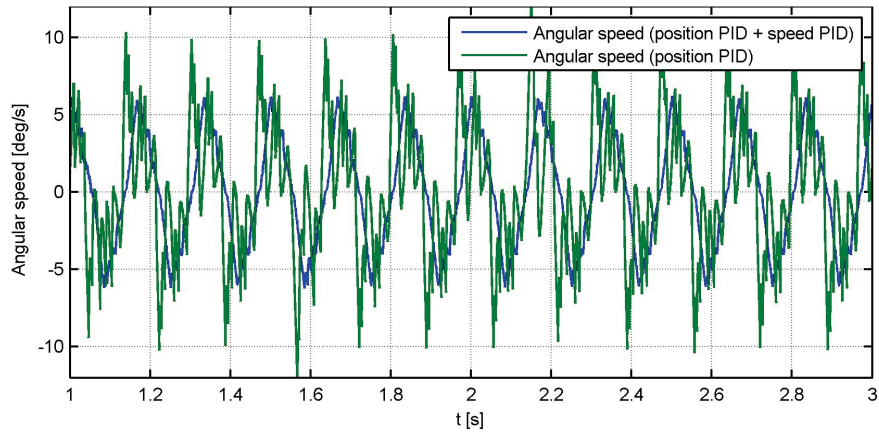


Figure 10 Angular speed of position controller and combined position + speed controller

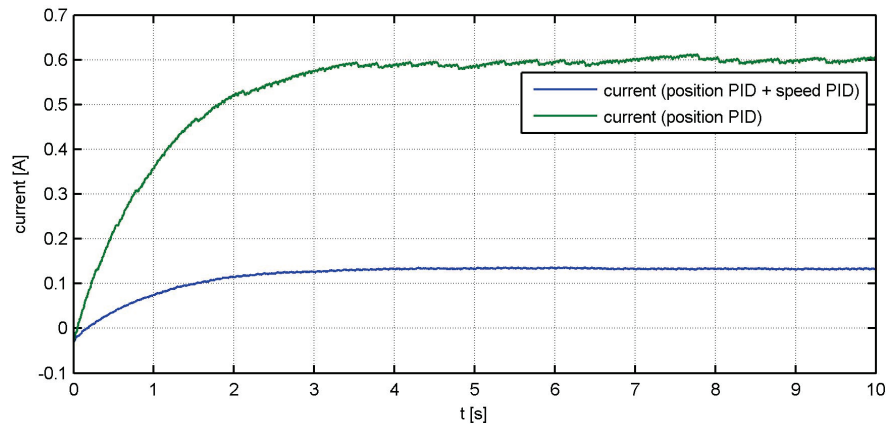


Figure 11 Current consumption from battery in case of position controller combined position + speed controller

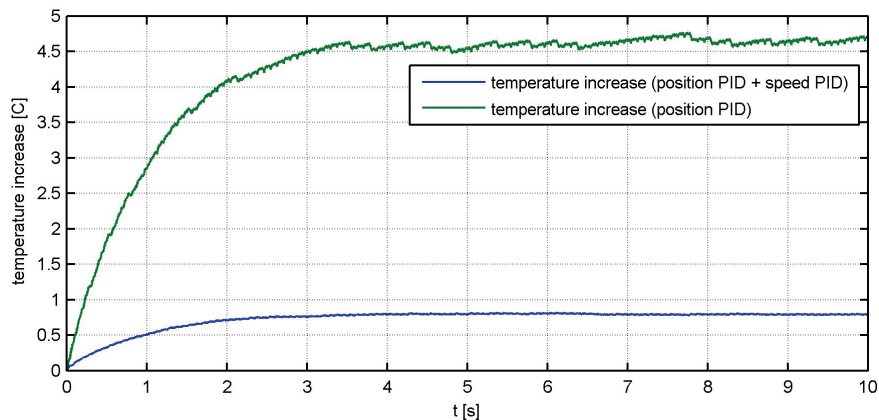


Figure 12 Heating in DC brushless motor in case of position controller and combined position + speed controller

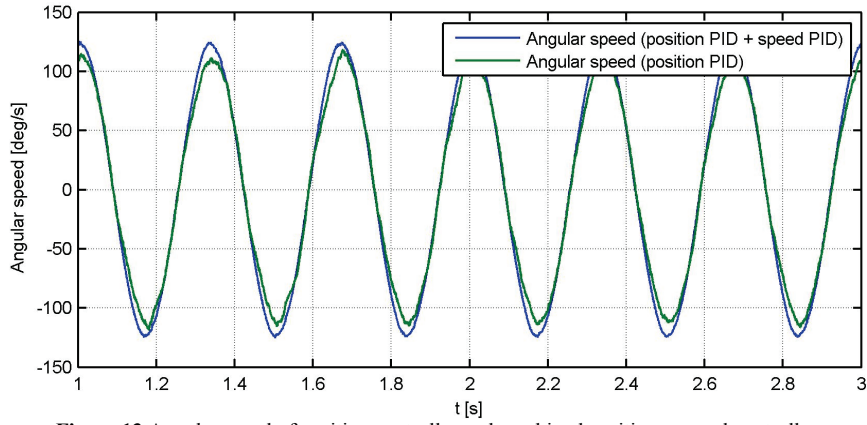


Figure 13 Angular speed of position controller and combined position + speed controller

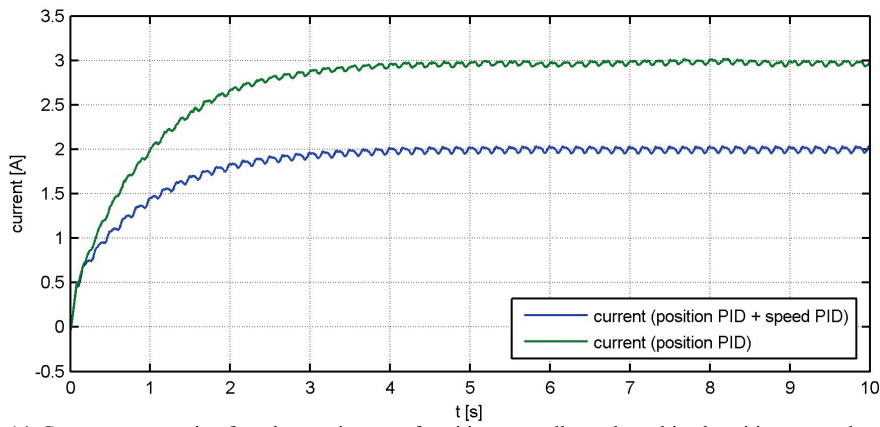


Figure 14 Current consumption from battery in case of position controller and combined position + speed controller

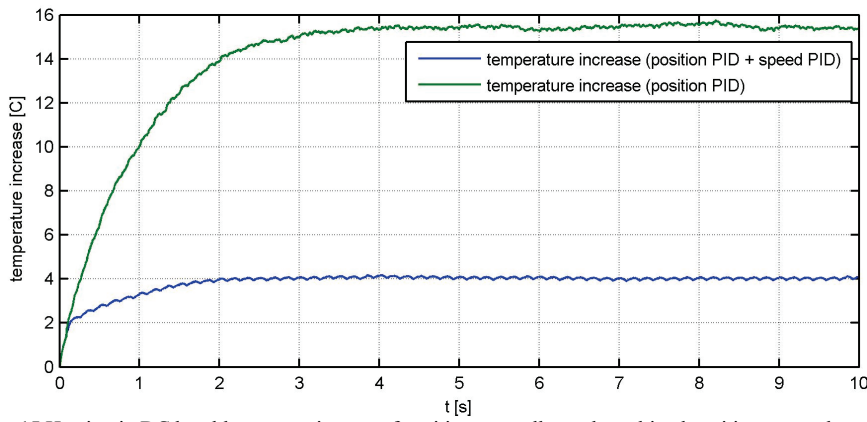


Figure 15 Heating in DC brushless motor in case of position controller and combined position + speed controller

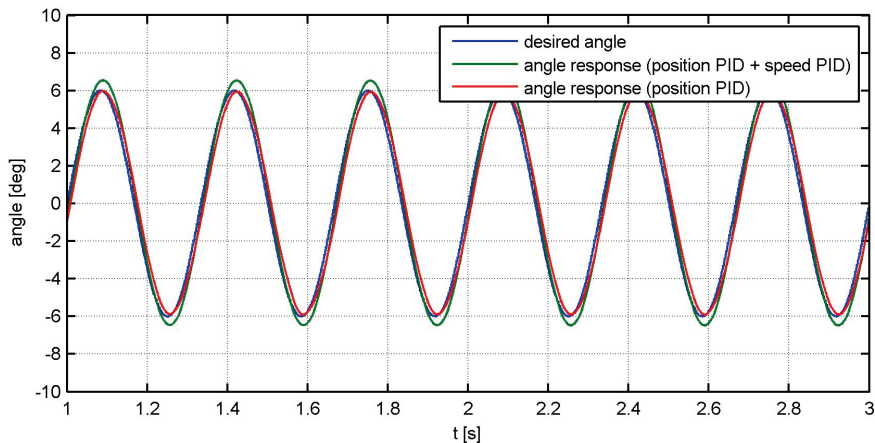


Figure 16 Angle response of position controller and combined position + speed controller

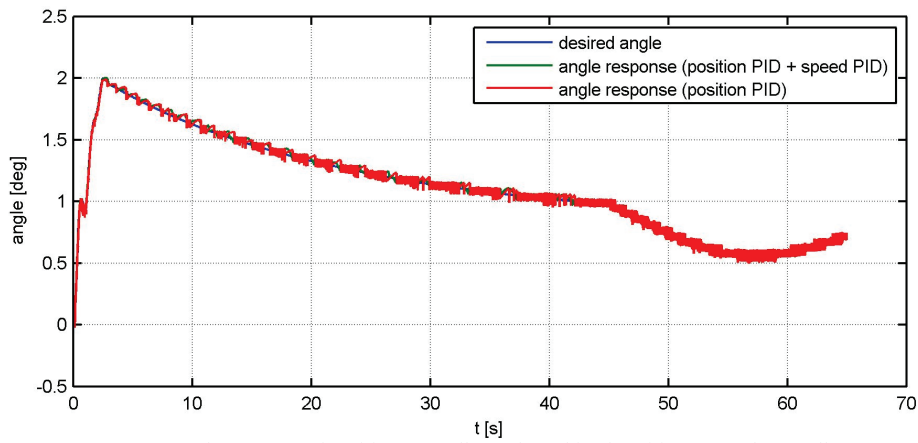


Figure 17 Angle response of position controller and combined position + speed controller

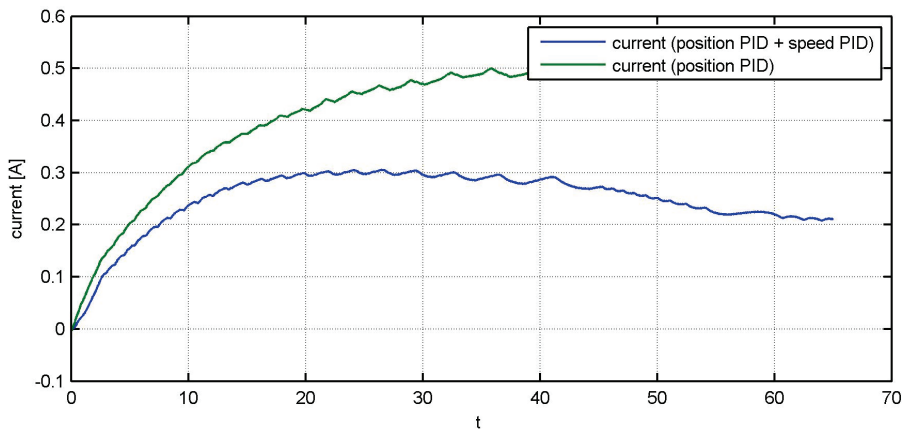


Figure 18 Current consumption from battery in case of position controller and combined position + speed controller

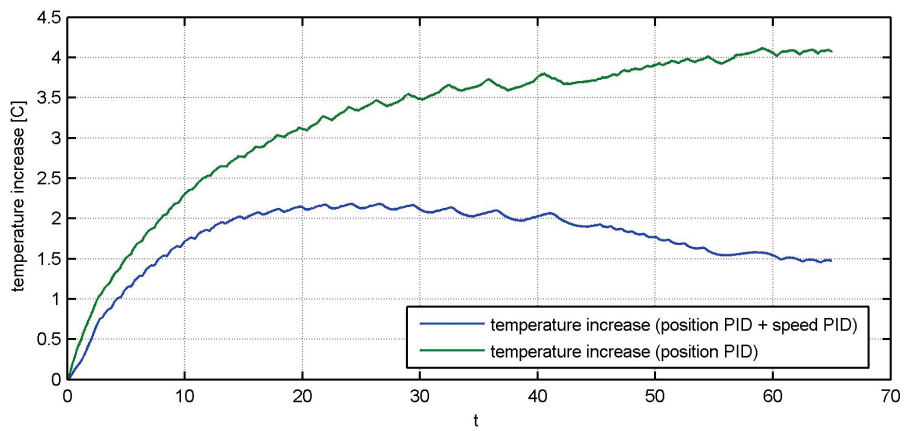


Figure 19 Heating in DC brushless motor in case of position controller and combined position + speed controller

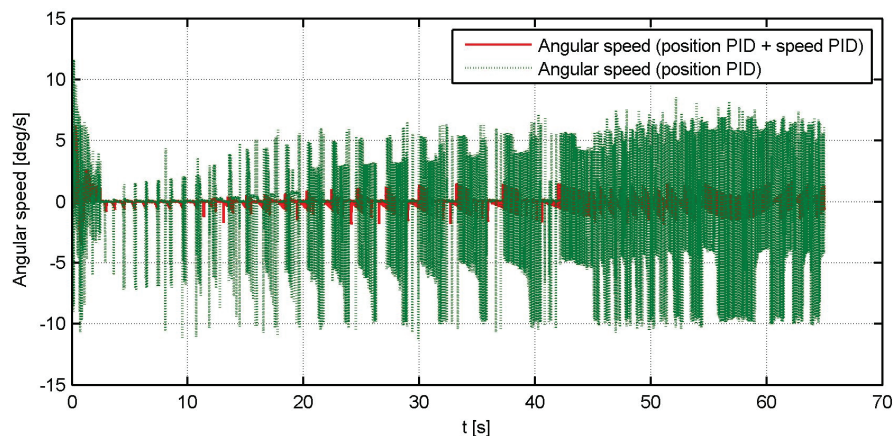


Figure 20 Angular speed of position controller and combined position + speed controller

6 Conclusions

Having in mind obtained results, one can conclude that:

- Small signal bandwidth of both types of regulation will be the same but response of combined regulator will be smoother;
- On maximum requirements, combined regulation can produce more overshoot, but in aerospace application that type of signal will never be used in real situation;
- Combined regulation generates less noise for lower level of errors;
- Results show that by using combined controller we can reduce current consumption from battery. That will have as a benefit less heating in the system and possibility of longer flight for the same power supply in one system;
- Control alternation (change of type of control) could be done in software code – no hardware change needed.

7 References

- [1] Cowan, J. R.; Myers, W. N. Design of High Power Electromechanical Actuator for Thrust Vector Control // 27th Joint Propulsion Conference / Sacramento, CA, U.S.A., 1991, AIAA 91-1849.
- [2] Weir, R.A.; Cowan, J.R. Development and Test of Electromechanical Actuators for Thrust Vector Control // 29th Joint Propulsion Conference / Monterey, CA, U.S.A., 1993, AIAA 93-2458.
- [3] Marinković, Z.; Marinković, D.; Petrović, G.; Milić, P. Modelling and Simulation of Dynamic Behaviour of Electric Motor Driven Mechanisms. // Tehnicki vjesnik-Technical Gazette. 19, 4(2012), pp. 717-725.
- [4] Grenier, D.; Dessaint, L. A.; Akhrif, O.; Bonnassieux, Y.; LePioufle, B. Experimental Nonlinear Torque Control of a Permanent-Magnet Synchronous Motor Using Saliency. // IEEE Transactions on Automatic Control. 44, 5(1997), pp. 680-687.
- [5] Trounce, J. C.; Round, S. D.; Duke, R. M. Evaluation of Direct Torque Control using Space Vector Modulation for Electric Vehicle Applications. University of Canterbury, New Zealand, 2001.
- [6] Chiasson, J. IEEE Press Series on Power Engineering: Modeling and High-Performance Control of Electric Machines, Wiley-IEEE Press, New York, USA, 2005.
- [7] Hansellman, D. C. Brushless Permanent Magnet Motor Design, McGraw-Hill, 1994.
- [8] McClure, M. A Simplified Approach to DC Motor Modeling for Dynamic Stability Analysis. // Application Report SLUA076, Texas Instruments, USA, 2000.
- [9] Schinstock, D. E.; Haskew, T. A. Identification of Continuous-Time, Linear, and Nonlinear Models of an Electromechanical Actuator. // Journal of Propulsion and Power. 13, 5(1997), pp. 683-691.
- [10] Schinstock, D. E.; Scott, D. A.; Haskew, T. A. Modeling and Estimation for Electromechanical Thrust Vector Control of Rocket Engines. // Journal of Propulsion and Power. 14, 4(1998), pp. 440-447.
- [11] Khan, M. A.; Todić, I.; Miloš, M.; Stefanović, Z.; Blagojević, Dj. Control of Electro-Mechanical Actuator for Aerospace Applications. // Strojarstvo. 52, 3(2010), pp. 303-313.

Authors' addresses

M.Sc. Ivana Todić, Assistant Lecturer

University of Belgrade, Faculty of Mechanical Engineering
Kraljice Marije 16, 11000 Belgrade, Serbia
E-mail: ivana.todic@gmail.com

Dr Marko Miloš, Associate Professor

University of Belgrade, Faculty of Mechanical Engineering
Kraljice Marije 16, 11000 Belgrade, Serbia
E-mail: mmilos@mas.bg.ac.rs

Dr Mirko Pavišić, Associate Professor

University of Belgrade, Faculty of Mechanical Engineering
Kraljice Marije 16, 11000 Belgrade, Serbia
E-mail: mpavistic@mas.bg.ac.rs